Boundary-Layer Meteorol (2015) 156:349–370
DOI 10.1007/s10546-015-0030-z

ARTICLE

Impact of Nocturnal Low-Level Jets on Near-Surface Turbulence Kinetic Energy

Henrique F. Duarte[1,3] · Monique Y. Leclerc[1] · Gengsheng Zhang[1] · David Durden[1] · Robert Kurzeja[2] · Matthew Parker[2] · David Werth[2]

Received: 21 July 2014 / Accepted: 14 April 2015 / Published online: 7 May 2015

Abstract We report on the role of low-level jets (LLJs) on the modulation of near-surface turbulence in the stable boundary layer, focusing on the behaviour of the transport terms of the turbulence kinetic energy (TKE) budget. We also examine the applicability of Monin–Obukhov similarity theory (MOST) in light of these terms. Using coincident near-surface turbulence and LLJ data collected over a three-month period in South Carolina, USA, we found that turbulence during LLJ periods was typically stronger and more well-developed in comparison with periods without a LLJ. We found a local imbalance in the near-surface TKE budget, in which the imbalance (residual) term was typically positive (i.e., energy gain) and nearly in equilibrium with buoyant consumption. Based on a comparison with previous studies, we assume that this residual term represents mostly pressure transport. We found the behaviour of the residual term to be better delineated in the presence of LLJs. We found shear production to adhere to MOST remarkably well during LLJs, except under very stable conditions. Gain of non-local TKE via pressure transport, likely consisting of large-scale fluctuations, could be the cause of the observed deviation from the MOST z-less prediction. The fact that this deviation was observed for periods with well-developed turbulence with an inertial subrange slope close to $-5/3$ indicates that such Kolmogorov turbulence is not a sufficient condition to guarantee the applicability of the MOST z-less concept, as recently suggested in the literature. The implications of these results are discussed.

Keywords Low-level jet · Monin–Obukhov similarity · Nocturnal stable boundary layer · Pressure transport term · Turbulence kinetic energy budget · z-Less turbulence

✉ Henrique F. Duarte
h.duarte@utah.edu

1 Laboratory for Atmospheric Biogeosciences, The University of Georgia, Griffin, USA

2 Savannah River National Laboratory, Aiken, USA

3 Present Address: Department of Atmospheric Sciences, Land-Atmosphere Interactions Research Group (LAIR), The University of Utah, 135 S 1460 E, RM 713 WBB, Salt Lake City, UT 84112, USA

1 Introduction

Low-level jets (LLJs) are a common feature of the nocturnal stable boundary layer (SBL) (Song et al. 2005; Karipot et al. 2009), and have been observed at numerous locations over all continents (e.g., May 1995; Banta et al. 2002; Vera et al. 2006; Todd et al. 2008; Karipot et al. 2009; Foken et al. 2012; Wang et al. 2013a). During nighttime over land, the formation of LLJs is typically associated with inertial oscillations (Blackadar 1957), while baroclinicity, katabatic flows, and frontal systems are some of the other possible causes of LLJ formation (Stull 1988).

LLJs have been associated with the long-range transport of scalars (e.g., Corsmeier et al. 1997; Sogachev and Leclerc 2011; Hong et al. 2012). They are often a significant source of turbulence in the nocturnal SBL given the enhanced shear created in the sub-jet layer (e.g., Mahrt et al. 1979; Mahrt 1999; Mahrt and Vickers 2002; Banta et al. 2002, 2003, 2006; Karipot et al. 2006, 2008; Duarte et al. 2012). Their potential to transport scalars (e.g., CO_2, H_2O, O_3, and pollutants) over hundreds of kilometres during a single night and to modulate near-surface turbulence and fluxes, coupled with their ubiquitous nature, underscores the relevance of LLJs to both the air pollution and eddy-flux communities (Corsmeier et al. 1997; Karipot et al. 2006, 2008; Sogachev and Leclerc 2011).

The turbulence kinetic energy (TKE) budget equation for a coordinate system aligned with the mean wind, assuming zero subsidence, is given by (Stull 1988),

$$\underbrace{\frac{\partial \bar{e}}{\partial t}}_{S_{\mathrm{tg}}} = \underbrace{-\bar{u}\frac{\partial \bar{e}}{\partial x}}_{A} \underbrace{+\frac{g}{\overline{\theta_{\mathrm{v}}}}\overline{w'\theta'_{\mathrm{v}}}}_{B} \underbrace{-\overline{u'w'}\frac{\partial \bar{u}}{\partial z}}_{S_{\mathrm{hr}}} \underbrace{-\frac{\partial \overline{w'e}}{\partial z}}_{T_{\mathrm{t}}} \underbrace{-\frac{1}{\bar{\rho}}\frac{\partial \overline{w'p'}}{\partial z}}_{T_{\mathrm{p}}} \underbrace{-\varepsilon}_{D} \tag{1}$$

where S_{tg} is the storage term, A is the advection term, B is the buoyant production/consumption term, S_{hr} is the shear production term, T_{t} is the turbulent transport term, T_{p} is the pressure transport term, D is the dissipation term, e is the instantaneous TKE, g is the acceleration due to gravity, θ_v is the virtual potential temperature, w is the vertical velocity component, u is the streamwise velocity component, ρ is the air density, p is the atmospheric pressure, and ε is the dissipation rate of TKE. The partial derivatives $\partial/\partial t$, $\partial/\partial x$, and $\partial/\partial z$ are with respect to time, streamwise direction, and vertical direction, respectively. Overbars indicate averaging and primes indicate fluctuations from the mean. The instantaneous TKE is given by $e = 0.5\left(u'^2 + v'^2 + w'^2\right)$, where v is the lateral velocity component.

A dimensionless version of Eq. 1 can be obtained by multiplying each term by $\kappa(z-d)/u_*^3$, where κ is the von Kármán constant, z is the height above the surface, d is the displacement height, and u_* is the friction velocity,

$$S_{\mathrm{tg}}^{+} = A^{+} + B^{+} + S_{\mathrm{hr}}^{+} + T_{\mathrm{t}}^{+} + T_{\mathrm{p}}^{+} + D^{+}. \tag{2}$$

Note that $B^{+} \equiv \kappa(z-d)B/u_*^3 = -\zeta$, where ζ is the Monin–Obukhov stability parameter.

The TKE budget in the surface layer has been studied within the framework of Monin–Obukhov similarity theory (MOST) for many years (Wyngaard and Coté 1971; Högström 1990; Oncley et al. 1996; Frenzen and Vogel 2001; Li et al. 2008). However, as Li et al. (2008) pointed out, many uncertainties still remain, especially on the role played by the transport terms. The classical assumption is that the TKE budget is locally balanced, i.e. the transport terms are either negligible or they cancel each other (McBean and Elliot 1975; Wyngaard 2010). However, experimental results have challenged this assumption, showing evidence of local imbalance and underscoring the importance of the transport terms (e.g., Högström 1990, 1992; Frenzen and Vogel 2001; Li et al. 2008). These studies have reported cases of

either excess or insufficient local dissipation, being associated with either TKE gain or loss via the transport terms respectively. The reason for these differences is still an open question (Li et al. 2008). This is especially true in the SBL, where turbulence is affected by LLJs, gravity waves, density currents, and Kelvin-Helmholtz shear instability (Cheng et al. 2005).

The TKE budget in the atmospheric boundary layer under the effect of LLJs was investigated in a few observational studies (Table 1). These studies were conducted for different sites, jet types, and stability conditions, and show that pressure transport plays an important role in the budget near the surface, but at present, there does not appear to be a consensus on whether the pressure transport term acts as a sink or source term.

Smedman et al. (1993, 1994) used aircraft slant profile data collected over the Baltic Sea (near the south-eastern Swedish coast) in their analysis. LLJs were present at heights from 500 to 1500 m, formed by frictional decoupling of the flow due to low sea surface temperatures (a process analogous to the formation of a nocturnal LLJ over land), and stability was near-neutral. In Smedman et al. (1993), the pressure transport term was found to be an important source term in the layer from the base to the top of the LLJ, with larger values at the base of the LLJ, where shear production was a maximum. In the particular case analyzed by Smedman et al. (1994), maximum shear production was also observed at the base of the LLJ, but in the same layer the pressure transport term was a sink. At lower layers down to the surface, the latter was a large source term. They suggested that the pressure transport term was responsible for transporting TKE from the layer of maximum shear production (at the jet base) down to the surface, and also suggested that the turbulence transported towards the surface was 'inactive' turbulence (large-scale fluctuations—see Högström 1990), helping to promote mixing in the sub-jet layer but not producing shear stress directly.

At a different site over the Baltic Sea (Stockholm archipelago), Smedman et al. (1995) analyzed the TKE budget for cases characterized by weak to moderate stability and lower-level LLJs (cores at 30 to 150 m above sea level). Tower data collected at 8 and 31 m above the surface were used, and maximum shear production was found closer to the surface (8-m level), and at the same level the pressure transport term was a sink. At the 31-m level the latter was a source term. They concluded that TKE was transported upwards by the pressure transport term, away from the layer of maximum shear production (in agreement with Smedman et al. 1994).

Bergström and Smedman (1995) used data from the same site (Smedman et al. 1995) and analyzed the TKE budget for cases with similar stability but *without* the presence of a LLJ. They found the pressure transport term to be a source at the 8-m level, and suggested that this was the result of the transport of 'inactive' turbulence from upper regions in the boundary layer towards the surface. Contrary to the pressure transport term, the turbulent transport term was found to be small in the studies discussed so far (Smedman et al. 1993, 1994, 1995; Bergström and Smedman 1995).

Over land (south-eastern Kansas, USA), Cuxart et al. (2002) also found significant values for the pressure transport term in the near-surface TKE budget for a night characterized by strong stratification and LLJ activity (jet height from 100 to 200 m above ground level, a.g.l.). They observed that, in a layer from 1.5 to 30 m a.g.l., the pressure transport was a relevant sink, coinciding with maximum shear production. In a layer from 30 to 50 m a.g.l., the pressure transport was a relevant source term. As in Smedman et al. (1995), the results of Cuxart et al. (2002) indicate that TKE was exported away from a layer of maximum shear production near the surface by the pressure transport term. Cuxart et al. (2002) observed significant values for the turbulent transport term as well, but its behaviour was not well-defined (i.e., regarding the orientation of the transport, away from or towards the surface).

Table 1 Observational studies reporting results on the pressure and turbulent transport terms (T_p and T_t respectively) of the TKE budget during (no-)LLJ conditions

Study	Location	Jet formation	Jet height (m)	Near-surface stability	Data type	T_p	T_p calculation	T_t
Smedman et al. (1993)	Baltic Sea, south-eastern Sweden	Frictional decoupling over the cold sea	500–1200	Near neutral	Aircraft slant profile	Gain at the top and base of the jet; larger values at the base (max S_{hr})	Residual	Very small (heights above/below the jet)
Smedman et al. (1994)	Baltic Sea, south-eastern Sweden	Frictional decoupling over the cold sea	≈1500	Near neutral	Aircraft slant profile + tower	Loss at the base of the jet (max S_{hr}); gain at lower layers down to the surface	Residual	Mostly small, changing sign at several heights
Smedman et al. (1995)	Baltic Sea, Stockholm archipelago	Frictional decoupling over the cold sea	30–150	Weakly to moderately stable	Tower	Loss at 8 m (max S_{hr}); gain at 31 m	Residual	Very small at 8 and 31 m
Bergström and Smedman (1995)	Baltic Sea, Stockholm archipelago	*No jet*	–	Weakly stable to very stable	Tower	Gain at 8 m	Residual	Very small at 8 m
Cuxart et al. (2002)	South-eastern Kansas, USA	Frictional decoupling at nighttime	100–200	Very stable	Tower	Loss at 1.5–30-m layer (max S_{hr}) and gain at 30–50-m layer	Direct	Significant at 1.5–30-m and 30–50-m layers, but not well-defined sign
Current study	Upper coastal plains of South Carolina, USA	Frictional decoupling at nighttime; baroclinicity	120–560	Weakly stable to very stable	Tower	Gain at 34–68-m layer	Residual	Very small at 34–68-m layer

Heights are given in metres above the surface. S_{hr} and D correspond to the shear production and dissipation terms, respectively

The TKE budget under LLJ conditions has also been studied based on numerical simulation data (e.g., Skyllingstad 2003; Muñoz and Garreaud 2005; Conangla and Cuxart 2006; Cuxart and Jiménez 2007; Axelsen and Dop 2009). Modelling approaches included the MM5 mesoscale model, single-column models, and large-eddy simulation. The two transport terms in these studies were practically negligible at layers below and above the jet, i.e., the TKE budget was practically locally balanced. Skyllingstad (2003) and Axelsen and Dop (2009) modelled katabatic flow (jet peak a few metres away from the surface), and found more substantial values for the pressure transport term. It is important to emphasize that the modelling of highly stratified flows is complex, and differences in the result for the transport terms may be simply related to the different modelling approaches and associated parametrizations and simplifications used.

As mentioned previously, the classical assumption is that the near-surface TKE budget is locally balanced, and therefore eventual gains or losses of TKE via the transport terms are expected to result in deviations from MOST. As discussed above, this is a concern especially in the SBL, where near-surface turbulence can be affected by many non-local processes. The applicability of MOST in the presence of LLJs has been discussed in a few studies. Smedman et al. (1995) observed a significant departure from MOST for their dimensionless wind-speed and temperature gradients measured near the surface (8 m) during conditions of weak to moderate stability in the presence of LLJs propagating at low heights (30–150 m) over the Baltic Sea. At the same site and under similar stability, but in the absence of LLJs, Bergström and Smedman (1995) found those dimensionless gradients to adhere to MOST. In Smedman et al. (1995), pointed out that the flow was significantly governed by the proximity of the jet to the surface, being similar to a laboratory wall jet. It is interesting to note that their results show a locally imbalanced TKE budget at the 8-m level, with a large loss of TKE via pressure transport.

In contrast with Smedman et al. (1995), Cheng et al. (2005) found dimensionless gradients of wind speed and temperature near the surface ($\approx$3 m) to follow MOST very well during the well-developed stage of a more typical type of LLJ over land (data from a particular night from CASES-99—Great Plains of the United States). The jet was observed at approximately 150 m a.g.l. and near-surface conditions were weakly stable. More recently, Banta et al. (2006) and Banta (2008) analyzed data from the CASES-99 and LAMAR-2003 experiments (strong-wind-speed nights characterized by weak to moderate stability) and found results in apparent conflict with local similarity concepts, as jet speed was found to be a more appropriate velocity scale than surface-layer friction velocity.

The studies referred to above indicate that the behaviour of the transport terms (especially the pressure transport term) and the applicability of MOST are still an open question in the SBL in the presence of LLJs. The results reported so far are practically based on case studies. Further studies using larger datasets encompassing a larger variety of jet and stability conditions are needed for a better understanding of the impact of LLJs on near-surface turbulence.

Addressing the question above, the goal of our study is to investigate the role of LLJs on the modulation of near-surface turbulence in the SBL over land, focusing on the behaviour of the transport terms of the TKE budget, and the applicability of MOST. Flux-tower and acoustic remote sensing data collected over a three-month period in South Carolina, USA are used in the analysis.

Section 2 presents information on the experimental site, instrumentation, data selection, and the processing of turbulence and acoustic remote sensing data. Results and discussion are presented in Sect. 3, starting with a characterization of the LLJ events analyzed (Sect. 3.1),

followed by the analysis of the TKE budget and the applicability of MOST (Sect. 3.2). Conclusions are presented in Sect. 4.

2 Measurements and Data Processing

2.1 Experimental Site and Instrumentation

Turbulence data were collected on a tall tower near Beech Island, South Carolina (33°24′20.18″N, 81°50′01.96″W, alt. 117 m) in 2009 and 2010. The region is characterized by a mosaic of broken forests (mixed pine) and agricultural lands, with urban, suburban, and industrial areas within 20 km (Fig. 1). Eddy-covariance measurements (three-dimensional wind velocity components, sonic temperature, and concentrations of CO_2 and water vapour) were made at 34, 68, and 329 m a.g.l. on the tall tower (Fig. 2) with three-dimensional sonic anemometers (Applied Technologies Inc., model Sx at 34 m, model A at 68 and 329 m; Longmont, Colorado, USA) and CO_2/H_2O gas analyzers (Li-Cor Inc., model Li-7500, Lincoln, Nebraska, USA) at a frequency of 10 Hz.

Vertical profiles of mean wind speed and direction, vertical velocity component, echo strength, and standard deviations of wind direction and velocity components were measured using a phased-array boundary-layer Doppler sodar (Remtech Inc., model PA2, Paris, France) operating with a central frequency of 2 kHz. The sodar was operated with a maximum vertical range of 1200 m, a vertical resolution of 20 m, and was programmed to retrieve 15-min averaged profiles. The sodar was deployed at the Savannah River Site (33°20′22.83″N, 81°33′51.40″W, alt. 87 m), near Aiken, South Carolina, approximately 26 km from the tall tower (Fig. 1). The sodar site is surrounded by mixed forest spanning several kilometres in all directions.

2.2 Data Selection

We selected the months of May, June, and July 2009 for the present study, and considered only nighttime data (2000 to 0500 Eastern Standard Time, EST). Several nights during these months presented LLJ activity lasting for multiple hours, with a high incidence of south-westerly winds. Continuous LLJ activity, formed by (or facilitated by) the stabilization of the atmospheric boundary layer on the regional scale, was a desired feature given the fact that the sodar and tall tower were separated by 26 km. South-westerly flow was also a desired feature, given the orientation of the sonic anemometers on the tall tower (210° azimuth). Winter months were avoided due to the predominance of north-easterly winds (direction in which turbulence is most disturbed by the tower structure).

2.3 Turbulence Data Processing

We processed the turbulence data in 30-min blocks, and used the despiking method described by Vickers and Mahrt (1997) and applied the planar-fit coordinate rotation described by Wilczak et al. (2001) to the wind velocity components. The data were then linearly detrended (Rannik and Vesala 1999). Resulting fluctuations were used to calculate variances and covariances, and only runs with average wind direction between 070° and 350° were considered to avoid flow distortion due to the tower structure (sonic anemometers were pointed to 210°).

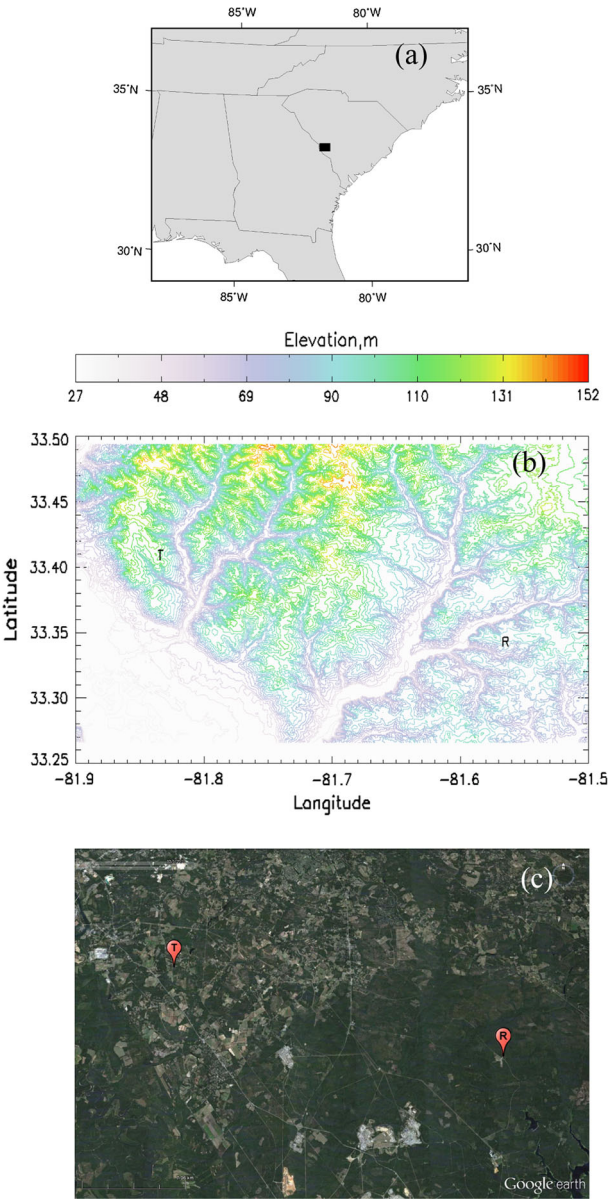

Fig. 1 **a** Site location in the USA, **b** local topography map, and **c** local satellite view (*source* Google Earth; imagery date: October 5 2010) showing land use. The location of the tall tower (T) and the Remtech sodar (R) are indicated

We calculated the dissipation rate of TKE (ε) by using the inertial dissipation method, based on Kolmogorov's hypothesis,

$$\varepsilon = \frac{2\pi}{\bar{u}} \left[\frac{f^{5/3} S_{uu}(f)}{\alpha_u} \right]^{3/2}, \tag{3}$$

Fig. 2 The Savannah River National Laboratory (SRNL) instrumented tall tower used in the study. The two lowest eddy-covariance systems (34- and 68-m levels) can be observed

where $\bar{u}$ is the average streamwise velocity component, $S_{uu}(f)$ is the spectral density of u as a function of natural frequency f, and α_u is the associated Kolmogorov constant, here taken as 0.5 (Batchelor 1953). In the inertial subrange, $f^{5/3}S_{uu}(f)$ is assumed to be constant, where $S_{uu} \propto f^{-5/3}$ (Kolmogorov's $-5/3$ power law). This method was also used in the Baltic Sea LLJ studies discussed in Sect. 1 (Smedman et al. 1993, 1994, 1995; Bergström and Smedman 1995).

The power spectrum of u was calculated for each 30-min run, and bin averaging was employed to smooth the spectra (64 non-overlapping f classes of logarithmically increasing width were used). We then used the frequency band $f[0.5 : 2.0]$ Hz to calculate the average of $f^{5/3}S_{uu}(f)$ and consequently ε via Eq. 3 (this frequency band was also used by Piper and Lundquist (2004) to calculate ε from similar sonic anemometer data).

Turbulence runs without a well-formed inertial subrange (i.e., presenting non-Kolmogorov turbulence) were removed from the analysis of the TKE budget terms and applicability of MOST. To be considered in the analysis, a given run was required to have an inertial subrange slope within the interval -1.69 ± 0.14 (note that $-5/3 = -1.67$), defined based on the average slope ± 2 standard deviations considering data from the 34- and 68-m levels during LLJs. This criterion led to the removal of 39/589 ($\approx$7 %) and 82/258 ($\approx$32 %) of the runs corresponding to the LLJ and no-LLJ events analyzed in this study (cf. Sect. 2.4), respectively. Turbulence in these removed runs was characterized by different degrees of non-stationarity.

2.4 Sodar Data Processing and LLJ Selection Criterion

The sodar data were averaged to 30-min profiles in order to allow the comparison with the tall-tower data. These 30-min profiles were used for selecting LLJ events. We used the same criterion used by Banta et al. (2002) for the identification of LLJs, where the first wind-speed maximum above ground level with speed at least 1.5 m s^{-1} larger than the adjacent minima above and below is classified as a LLJ. For each sodar profile, an automated routine was used to determine points of maximum and minimum wind speeds and to select a tentative LLJ height based on the 1.5 m s^{-1} criterion. Depending on the shape of the wind-speed profile, the determination of the points of maximum and minimum wind speeds—for the purpose of

Table 2 Statistics of the LLJ events (30-min profiles) observed from May to July 2009, 2000 to 0500 EST

	Avg ± SD [min:max]
Z_j (m)	326 ± 79 [120:560]
U_j (ms^{-1})	11.2 ± 2.6 [4.6:19.3]
U_j/Z_j (s^{-1})	0.035 ± 0.007 [0.018:0.058]
Number of events (LLJ)	700
Number of events (no-LLJ)	376
Number of profiles used in the analysis	1489
Number of 30-min blocks in the period of interest	1767

Each event is associated with continuous jet activity (minimum duration of 2 h). The number of continuous no-LLJ runs is also shown

LLJ height selection—is sometimes not trivial. We performed a visual inspection to verify, and if necessary correct, the selections from the automated routine. With this method, we extracted the relevant LLJ information—height (Z_j), speed (U_j), and direction (ϕ_j)—for the period of interest. Intermittent jets were not considered in this study (see discussion in Sect. 2.2). Only LLJs with duration ≥2 h (i.e., for a minimum of four consecutive 30-min profiles) were included in the 'LLJ group'. Similarly, continuous periods (≥2 h) without LLJ activity were also determined, providing a contrasting 'no-LLJ group' for comparison.

3 Results and Discussion

3.1 LLJ Statistics

Table 2 presents the statistics for the observed LLJs. The period of interest in this study spans from April 30 2009 (2000 EST) to August 1 2009 (0500 EST), only considering the 30-min blocks between 2000 and 0500 EST. The total number of 30-min blocks associated with this period is 1767, and the number of 30-min sodar profiles used in the analysis is 1489 (i.e., ≈84 % coverage). Sodar data were unavailable or of poor quality during the remaining periods.

Results show a high occurrence rate of LLJs at the experimental site during the months of May–July, where continuous jet activity was observed in 47 % of the profiles analyzed. Interestingly, Karipot et al. (2009) also reported in their climatological study a 47 % jet occurrence rate for their site also in south-eastern USA (northern Florida) for the months of June–August. It is important to note, however, that both continuous jets *and* intermittent jets were included in their statistics, while in the present study only continuous jets were considered. The results therefore suggest a higher occurrence rate of jets at the South Carolina site.

Figure 3 shows histograms of jet height, speed, and direction. For jet height, we can see higher frequencies in the 300–400-m range, especially at 380 m, while jet speed presents a frequency peak in the 10–13-m s^{-1} range. Regarding jet direction, we can see a higher occurrence in the south-west quadrant, especially between south-west and west. These results are in general agreement with the climatological results reported by Karipot et al. (2009) for their northern Florida site during summer months.

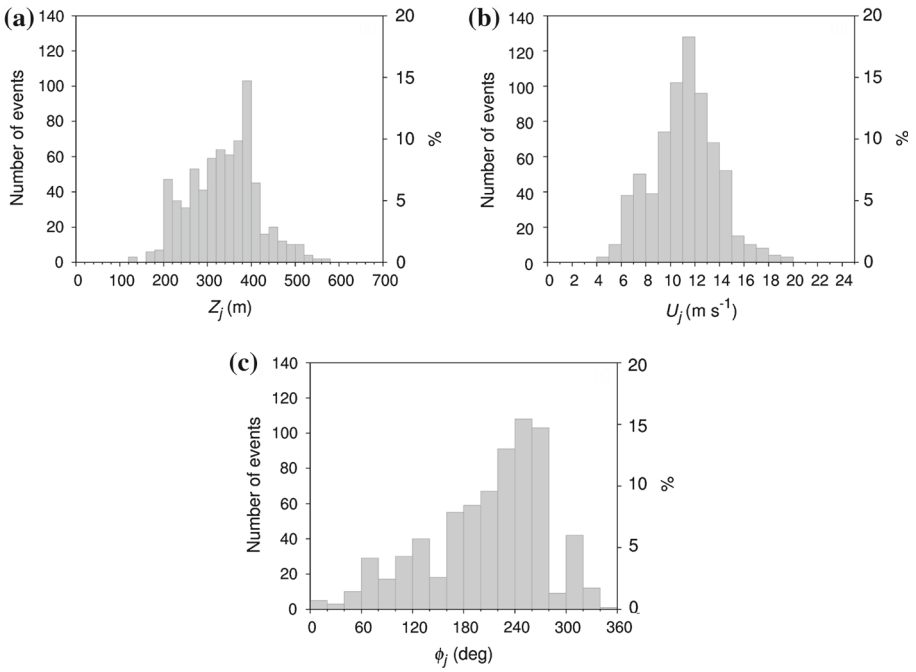

Fig. 3 Histograms of LLJ **a** height, **b** speed, and **c** direction for the 700 jet events (30-min profiles) observed from May to July 2009, 2000 to 0500 EST. These events are associated with continuous jet activity (minimum duration of 2 h)

In order to illustrate the general shape of the LLJs analyzed in this study, Fig. 4 presents a composite wind-speed profile for all selected cases (see Table 2). Note the well-defined linear behaviour in the sub-jet layer, with less scatter, and the relatively narrow LLJ core. This linear behaviour was also observed for the Great Plains LLJ (Banta et al. 2003, 2006). Interestingly, the results in Fig. 4 for $\bar{u}/U_j$ in the sub-jet layer are very similar to the results in Banta et al. (2006, Fig. 7c), even down to the intercept at the top of the surface layer ($\bar{u}/U_j \approx 0.35$). Such similarity, even with differences in terrain and climatology between the two experimental sites, suggests a generality of profile properties during LLJs, a fact of relevance to numerical simulation efforts.

Given the location of our experimental site in the upper coastal plains of South Carolina, and considering the proximity of the Appalachian Mountains and the Atlantic Ocean, terrain-induced baroclinicity along with inertial accelerations likely play an important role in the development of the south-westerly jets observed in this study. Pibal observations of the Carolina LLJ by Sjostedt et al. (1990) show a predominance of LLJs with direction parallel to the coastline, with a higher frequency of north-easterly jets during autumn and south-westerly/westerly jets during spring and summer (the case of the present study). Doyle and Warner (1993) investigated the structure and dynamics of the north-easterly Carolina LLJ using a mesoscale numerical model, and found that the jet is formed due to strong baroclinicity in the region between the Appalachian Mountains and the Atlantic Ocean, and that its strength is modulated by strong inertial accelerations. Observations from a site in Maryland (a mid-Atlantic state) during the warm season (Zhang et al. 2006) also indicate the predominance of south-westerly/westerly LLJs. Zhang et al. (2006) investigated the dynamics of the south-

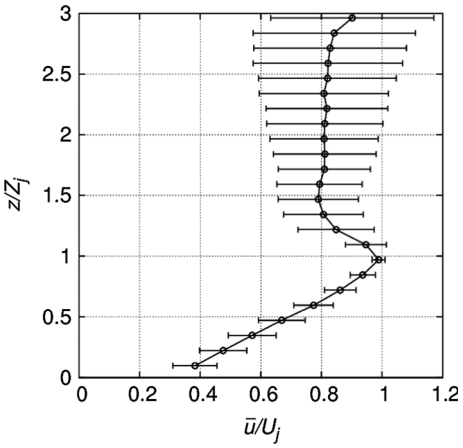

Fig. 4 Composite wind-speed profile for all LLJ events considered in this study. LLJ speed and height are used as scaling parameters. *Error bars* indicate ±1 standard deviation

westerly LLJ using a mesoscale numerical model, and as with Doyle and Warner (1993), found that baroclinicity (due to the Appalachians Mountains and the Atlantic Ocean) and inertial accelerations play an important role in the development of the LLJ.

3.2 TKE Budget

Except for the pressure transport and advection terms, we calculated all the budget terms directly (Eq. 1) for a layer between 34 and 68 m a.g.l. For the calculation of S_{tg}, B, and S_{hr}, we averaged the values of $\bar{e}$, $\overline{\theta_v}$, $\overline{w'\theta_v'}$, and $\overline{u'w'}$ observed at 34 and 68 m. The dissipation rate of TKE was calculated using Eq. 3, and the average ε between 34 and 68 m was used to calculate D in Eq. 1. A residual term was calculated as

$$R = S_{tg} - B - S_{hr} - T_t - D. \tag{4}$$

Note that R includes the sum of the pressure transport and advection terms, in addition to accumulated errors that may eventually occur in the calculation of the right-hand side of Eq. 4. In order to calculate the advection term directly, spatial measurements of TKE in the streamwise direction would be necessary, not easily accomplished with tower-based measurement platforms. Most studies usually neglect the term under the assumption of horizontal homogeneity. With regards to the pressure transport term, its direct calculation depends on accurate measurements of small fluctuations of static atmospheric pressure, which are extremely difficult to obtain with the available sensor technology. Given this issue, the residual approach, despite its limitations, has been widely used to investigate T_p (e.g., Högström 1990; Smedman et al. 1993, 1994, 1995; Bergström and Smedman 1995; Li et al. 2008).

Each term in Eq. 4 was non-dimensionalized according to Eq. 2, using $\kappa = 0.4$, $d = 13.2$ m, $z = 51$ m (34–68-m layer midpoint), and the average u_* between 34 and 68 m. According to MOST, those terms are expected to be a function of ζ. Figure 5a–d presents the normalized TKE budget terms as a function of ζ (i.e., the negative of the normalized buoyant production/consumption term, $-B^+$, calculated for the 34–68-m layer) for the selected LLJ events. The bin averages for each term are plotted together in Fig. 6. It can be seen that shear production and dissipation are the dominant terms of the budget, as expected in the SBL (Wyngaard 2010). The turbulent transport is found to be virtually zero (cf. Fig. 6), and the storage term is found to be negligible (data not shown). The results do not support, however, the concept of a locally-balanced TKE budget. Dissipation is found to have approximately

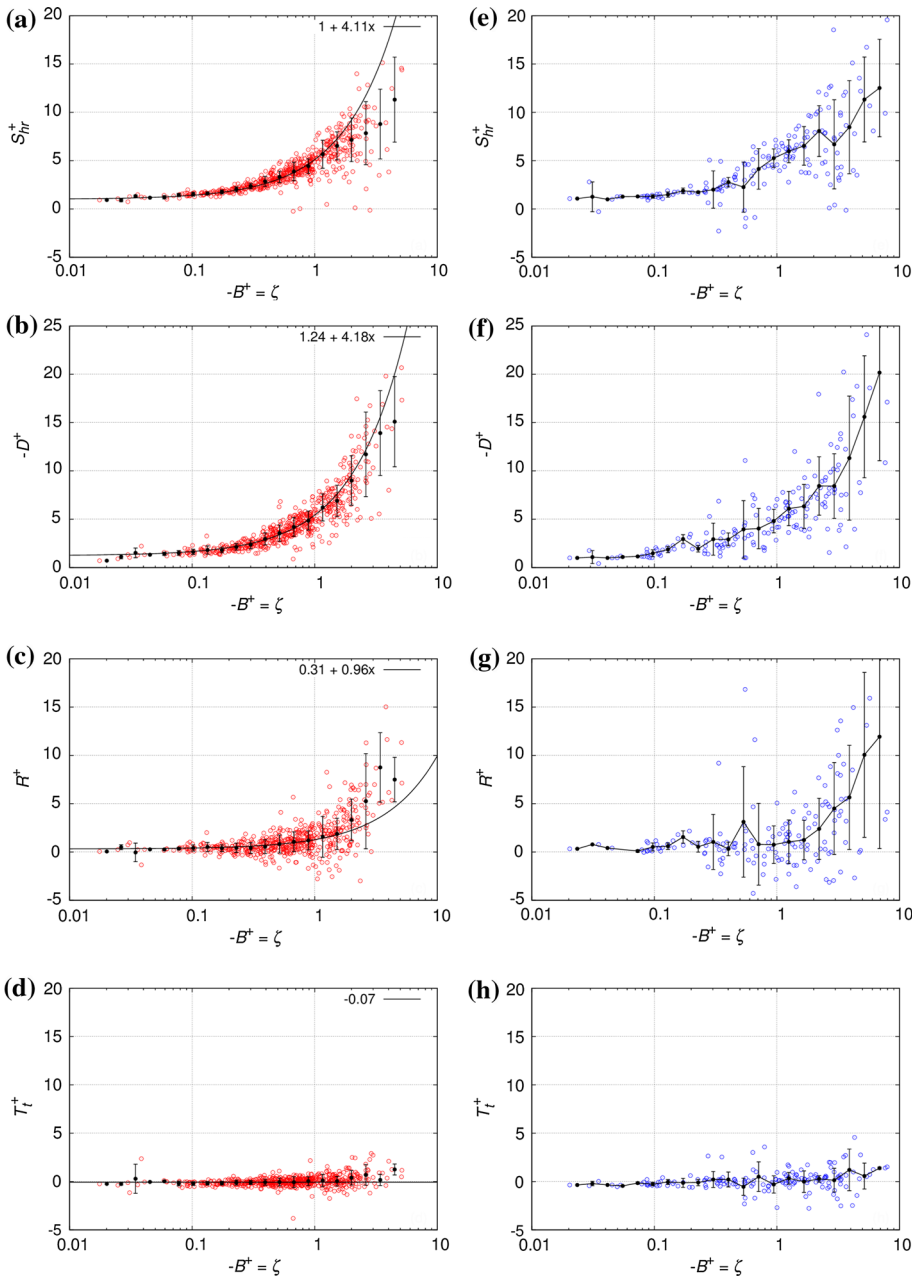

Fig. 5 Normalized TKE budget terms as a function of stability for the LLJ (*left column*, *red circles*) and no-LLJ (*right column*, *blue circles*) groups: **a**, **e** shear production, **b**, **f** dissipation, **c**, **g** residual, and **d**, **h** turbulent transport. *Black bullets* are bin averages, and *error bars* correspond to ± 1 standard deviation. *Curves on the left column* correspond to least-square fitting for data points up to $\zeta = 1$

the same magnitude as shear production, and the total local losses, i.e., $D + B$, therefore exceed the local production, indicating a gain of non-local TKE in the layer. This gain is represented by the residual term, which includes advection and pressure transport.

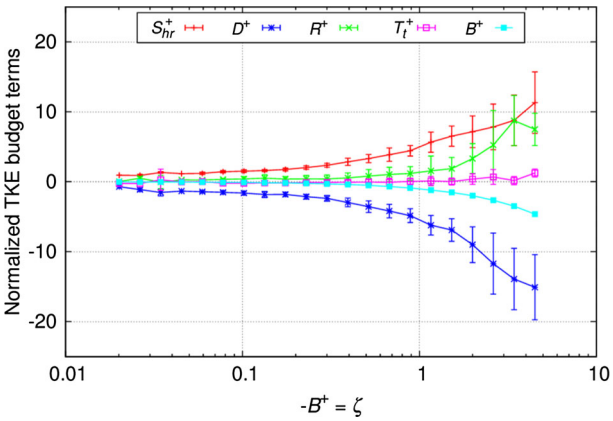

Fig. 6 Normalized TKE budget terms for the LLJ group. *Points* correspond to the bin averages shown in Fig. 5a–d. *Error bars* correspond to ±1 standard deviation

Despite the presence of several large positive values, we see from the bin-averaged values that, on average, R^+ is approximately in balance with buoyant consumption. Högström (1990) obtained similar results for a nearly-ideal site over land, flat and with a long uniform upwind fetch, in which the advection of TKE is expected to be negligible (or much reduced) and the residual term is expected to basically represent the pressure transport term (plus eventual accumulated errors). Even though our site characteristics are more complex, the fact that we observed similar results for R^+ may suggest that $R^+ \approx T_{\mathrm{p}}^+$ in our study as well. If the advection term is generally dominant, we expect R^+ to present a less systematic behaviour (energy gain/loss) in comparison to the results obtained. Also, the general result of $S_{\mathrm{hr}}^+ \approx -D^+$, $T_{\mathrm{t}}^+ \approx 0$, and $R^+ \approx -B^+$, assuming $R^+ \approx T_{\mathrm{p}}^+$, is in agreement with Kaimal and Finnigan (1994) regarding the TKE budget in the SBL.

It is important to note, however, that the advection term is expected to be larger and have a greater influence on R^+ during more stable conditions ($\zeta \gtrsim 1$), and the presence of a LLJ may help to accentuate the contribution of advection. Also, as mentioned previously, any accumulated error that may eventually result from the calculation of the budget terms on the right-hand side of Eq. 4 is reflected in the residual term. Similarly to the advection term, these errors are also expected to be larger and have a greater influence on R^+ during more stable conditions, where turbulence is weaker and more intermittent. It is also important to point out that different calculation methods (e.g., choice of Δz in the calculation of S_{hr}^+, turbulence data processing used to calculate fluxes) could potentially lead to different levels of error, with a direct impact on the residual term. In respect to the choice of the averaging period for calculating turbulent fluctuations, in this study we adopted the AmeriFlux standard (30 min), which could be argued to be too long for the study of turbulence in stable conditions. However, we investigated the impact of different averaging periods (30 vs. 5 min, data not shown) on the calculation of the major contributor to the TKE budget, i.e., shear production, and the general result was similar for both approaches.

The results show that S_{hr}^+ and D^+ terms follow MOST (local scaling formulation) remarkably well up to $\zeta \approx 1$ (Fig. 5a, b), corroborating earlier findings by Cheng et al. (2005). This result is in agreement with the concept of z-less stratification (i.e., turbulence statistics assumed to be independent of z). The z-less theory predicts a linear behaviour of those terms with ζ (Hong 2010; Grachev et al. 2013). The observed near-zero turbulent transport term

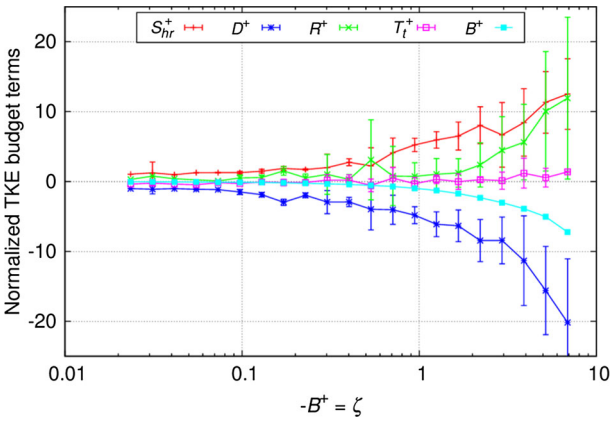

Fig. 7 Normalized TKE budget terms for the no-LLJ group. *Points* correspond to the bin averages shown in Fig. 5e–h. *Error bars* correspond to ±1 standard deviation

(Fig. 5d) is consistent with the concept of a locally-balanced TKE budget (cf. Sect. 1) and z-less stratification. Note that T_t^+ and T_p^+ represent the vertical divergence ($\partial/\partial z$) of the terms $-\overline{w'e}$ and $-\overline{w'p'}/\bar{\rho}$ respectively (cf. Eq. 1), which is expected to be null in z-less conditions. The non-zero residual term (Figs. 5c, 6), however, does not support the concept of local equilibrium ($R^+ \approx -B^+$). The concept of z-less stratification is also not supported, assuming that $R^+ \approx T_p^+$ at least for weakly to moderately stable conditions (as discussed previously). Further discussion on R^+, T_p^+ terms and the observed z-less breakdown is presented in Sect. 3.2.1.

The normalized TKE budget terms for the no-LLJ group are presented in Figs. 5e–h and 7. We see that the normalized TKE budget terms in both LLJ and no-LLJ groups follow practically the same behaviour, with greater scatter present for the no-LLJ points. In this group, even with the filtering method based on the inertial subrange slope values (cf. Sect. 2.3), some scatter still persists. This scatter is amplified for the residual term, whose behaviour is not as well-defined as for the LLJ group. Turbulence and flow properties for the LLJ and no-LLJ groups are compared below, helping to understand the differences observed in Figs. 5, 6 and 7 for the two groups.

The near-surface turbulence statistics in Table 3 show that for the LLJ group, average TKE and friction velocity are 30 and 39 % greater than for the no-LLJ group, respectively, and the average Monin–Obukhov stability parameter is 49 % smaller. Average streamwise velocity component and wind shear are 20 and 30 % greater for the LLJ group (also indicated by the histograms in Figs. 8 and 9), respectively. The differences of the median values between both groups are even more pronounced. Table 3 also shows larger standard deviations in the turbulence statistics observed for the no-LLJ group. Note that the S_{uu} inertial subrange slopes (β) for the LLJ group are close to the expected $-5/3$ value, while more scatter is observed for the no-LLJ group (57 % higher standard deviation), with a reasonably larger amount of runs being rejected by the filter described in Sect. 2.3. These results indicate that the no-LLJ cases are more susceptible to non-stationarity issues associated with lower wind speeds and weaker turbulence, while the LLJ cases tend to present stronger and more well-developed turbulence associated with greater wind speeds. We should also note that the no-LLJ periods are typically characterized by a larger cloud-cover fraction in comparison with the LLJ periods. Clouds may explain the non-formation of jets in some cases, given

Table 3 Near-surface turbulence statistics (34-m data) for the LLJ and no-LLJ groups, for ζ [0:10]

	LLJ	No-LLJ
	Avg $\pm$ SD [min:max], median	Avg $\pm$ SD [min:max], median
ζ	0.46 ± 0.63 [0.004:8.00], 0.29	0.91 ± 1.11 [0.004:8.29], 0.53
$\bar{e}$ (m^2 s^{-2})	0.35 ± 0.30 [0.01:1.96], 0.26	0.27 ± 0.46 [0.01:2.78], 0.12
u_*(m s^{-1})	0.25 ± 0.13 [0.02:0.72], 0.23	0.18 ± 0.15 [0.02:0.77], 0.13
$\bar{u}$ (m s^{-1})	3.15 ± 0.77 [0.31:5.84], 3.23	2.58 ± 1.04 [0.41:6.23], 2.36
$\Delta\bar{u}/\Delta z$(s^{-1})	0.052 ± 0.013 [-0.001:0.092], 0.052	0.040 ± 0.017 [-0.015:0.078], 0.041
β	-1.69 ± 0.07 [-1.88:-1.20], -1.70	-1.67 ± 0.11 [-1.93:-1.15], -1.70
N	591	240

$\Delta\bar{u}/\Delta z$ is the wind shear calculated between 34 and 68 m, and N is the number of 30-min runs in each group

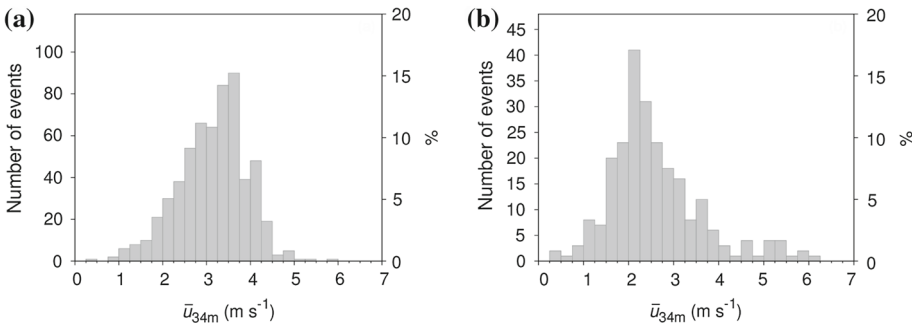

Fig. 8 *Histograms* of mean streamwise velocity component at 34 m for the **a** LLJ and **b** no-LLJ groups. Statistics are presented in Table 3

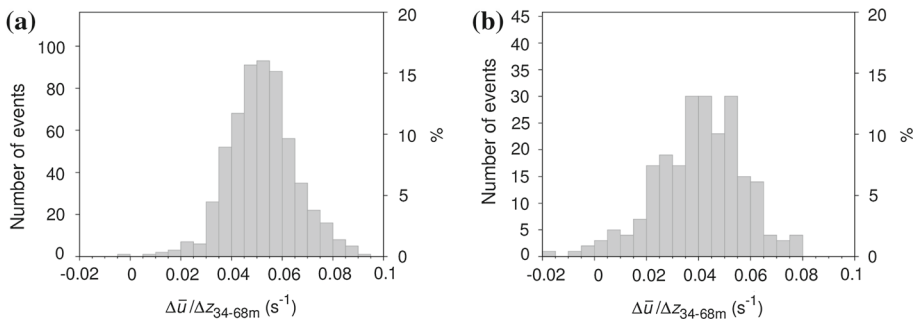

Fig. 9 *Histograms* of wind shear (calculated between 34 and 68 m) for the **a** LLJ and **b** no-LLJ groups. Statistics are presented in Table 3

their impact on the surface energy budget. Using ceilometer data collected at the Savannah River Site, we found a maximum cloud-cover fraction of [2.4 ± 2.7, 0.8] oktas for the LLJ events and [4.0 ± 2.8, 6.0] oktas for the no-LLJ events (avg $\pm$ SD, median).

Focusing on the results for the LLJ group, we fitted the following curves to the data in Fig. 5a, b, d,

$$S_{\mathrm{hr}}^{+} = 1 + c_1\zeta, \tag{5}$$
$$D^{+} = c_2 + c_3\zeta, \tag{6}$$
$$T_{\mathrm{t}}^{+} = c_4, \tag{7}$$

where c_1, c_2, c_3, and c_4 are constants. Equation 5 is the classical Businger-Dyer relation (Businger et al. 1971; Dyer 1974) for the dimensionless shear production term in stable conditions, and Eq. 6 corresponds to the typical form used for the dimensionless dissipation under the same conditions (Li et al. 2008). We only used data up to $\zeta = 1$ for the curve fitting, given the higher uncertainties at higher stabilities, finding

$$S_{\mathrm{hr}}^{+} = 1 + 4.11\zeta, \tag{8}$$
$$D^{+} = -1.24 - 4.18\zeta, \tag{9}$$

and

$$T_{\mathrm{t}}^{+} = -0.07. \tag{10}$$

With the results above, $R^{+}(0)$ must equal 0.31 in order to close the budget. We therefore fitted the following curve to the data in Fig. 5c,

$$R^{+} = 0.31 + c_5\zeta, \tag{11}$$

and obtained

$$R^{+} = 0.31 + 0.96\zeta. \tag{12}$$

The dimensionless shear production term in our study is reasonably close to the prediction [$c_1 = 4.11$ vs. 4.7 in Businger et al. 1971; we actually observed an even closer result when limiting the curve fitting to the data up to $\zeta = 0.5$ (results not shown)]. Our results also show an excess of dissipation, being associated with the input of non-local TKE via the pressure transport and advection terms (included in the residual term).

Similar results based on observations over land were reported by Högström (1990), who for weakly stable conditions found

$$S_{\mathrm{hr}}^{+} = 1 + 4.8\zeta, \tag{13a}$$
$$D^{+} = -1.24 - 4.7\zeta, \tag{13b}$$
$$T_{\mathrm{t}}^{+} = -0.25, \tag{13c}$$

and

$$T_{\mathrm{p}}^{+} = 0.49 + 0.9\zeta, \tag{13d}$$

with greater reliability for ζ up to 0.2, given the available data. The T_{p}^{+} term was calculated as a residual, and advection was assumed negligible for the near-ideal site. As discussed previously, the similarity between Eqs. 12 and 13d may indicate that our residual term represents mostly the pressure transport term, at least for conditions of weak to moderate stability. In a later study, Högström (1992) found for neutral conditions $D^{+}(0) = -1.24$, $T_{\mathrm{t}}^{+}(0) = 0$, and $T_{\mathrm{p}}^{+}(0) = 0.24$. These values are even closer to those found in the present study; the value we found for $D^{+}(0)$ is exactly the same as the one reported by Högström (1990, 1992).

Högström (1990) suggested that the observed near-surface energy gain via T_{p}^{+} was related to 'inactive' turbulence (large-scale fluctuations that do not promote the transport of momentum) being injected to the surface layer from the upper regions of the boundary layer. Smedman et al. (1994) found the same result at a different site and observed that TKE was transported away from a layer of strong shear production underneath a LLJ to the surface via pressure transport.

As alluded to earlier, other studies have also reported results indicating that T_p is a significant term in the near-surface TKE budget during LLJ conditions (cf. Table 1). These studies were associated with different sites, LLJ types, and stability levels, while the role of the pressure transport term as a sink or a source term varied in each study. Before comparing the results, it is important to emphasize once more the uncertainties associated with the calculation of T_p. The differences observed across studies could be at least in part related to different approaches used in its calculation, as discussed below.

In all studies cited in Table 1, except Cuxart et al. (2002), the pressure transport term was calculated as a residual. Again, note that this term may include advection (assumed negligible, but may vary from site to site) and accumulated errors from the calculation of other budget terms. Different choices of Δz for the calculation of the gradients, measurement types (tower vs. aircraft), turbulence data processing, and screening methods to remove unsuitable periods for the calculation of the dissipation term are factors that may lead to different levels of error and therefore to differences in T_p. On the other hand, Cuxart et al. (2002) calculated T_p directly, i.e., they used data from sonic anemometers and collocated microbarographs to obtain $\overline{w'p'}$. This approach, however, is known to be problematic due to the limitation of the available technology to measure small static pressure fluctuations of interest (Li et al. 2008).

The general result seen in Table 1 is that TKE is exported away from a layer of maximum shear production by the pressure transport term. This layer of maximum shear production can be near the surface (Smedman et al. 1995; Cuxart et al. 2002) or aloft near the base of the LLJ (Smedman et al. 1994), depending on the jet characteristics and stratification in the boundary regions. The former scenario corresponds to a traditional boundary layer, while the latter corresponds to an upside-down boundary layer (Mahrt and Vickers 2002). It is important to note, however, that the results obtained by Smedman et al. (1993) and Bergström and Smedman (1995) do not align with the general result discussed here. Smedman et al. (1993) found T_p to be consistently positive at the top and base of LLJs, while Bergström and Smedman (1995) found T_p to be positive near the surface in the absence of LLJs. These results indicate that the energy gain via T_p may be associated with a different process.

Assuming that our residual term represents mostly the pressure transport term, at least for conditions of weak to moderate stability, three possible explanations for the positive (gain) values we found for the 34–68-m layer during LLJ events are: (i) maximum shear production occurs near the surface, and TKE is transported upwards by T_p into the layer; (ii) maximum shear production occurs close to the LLJ, and TKE is transported downwards by T_p; and (iii) energy from the upper regions in the boundary layer is transported towards the surface layer, regardless of whether the maximum shear production occurs near the surface or aloft near the LLJ, in a process not necessarily associated with LLJs. Our results indicate typically higher turbulence intensities near the surface and decreasing magnitudes with height (not shown), suggesting the presence of a traditional boundary layer and supporting (i) instead of (ii). Explanation (iii) also seems to have value. The fact that we obtained approximately similar results for the no-LLJ group reinforces (i) and (iii). Note that gravity waves are expected to affect T_p, given the associated oscillations in static atmospheric pressure (Stull 1988). Bergström and Smedman (1995), for instance, found $T_p > 0$ near the surface for stable, no-LLJ conditions that coincided with evidence of gravity-wave activity for most of the events analyzed.

Even though our results show an approximately similar behaviour of R for both no-LLJ and LLJ groups, typically presenting positive values, the results indicate that R is better delineated in the presence of LLJs, where this term is in a closer balance with buoyant consumption. While the results in both groups could be possibly linked with gravity waves—which are a common phenomenon in the SBL—we hypothesize that gravity-wave activity

is more consistent during the LLJ events, leading to a more consistent behaviour of T_p. LLJs are known to promote the generation of gravity waves by shear-flow instability (e.g., Mastrantonio et al. 1976; Shuqing 1985; Wang et al. 2013b), given the fact that LLJs are associated with a stratified, stable flow and given the strong vertical wind shear they impose. It is important to note, however, that the less-consistent behaviour of R for the no-LLJ group is at least in part related to higher uncertainties in the calculation of the TKE budget terms due to the impact of non-stationarity. Further studies exploring this possible relationship between LLJs, gravity waves, and T_p are suggested.

3.2.1 Z-less Breakdown and T_p

As discussed in Sect. 3.2, the shear production term is found to adhere to MOST remarkably well up to $\zeta \approx 1$ (Fig. 5a), in agreement with the linear z-less prediction. Above $\zeta \approx 1$, S_{hr}^{+} is found to be typically smaller than the linear prediction, suggesting a breakdown of the z-less concept. This behaviour has also been reported in other studies (see review by Hong 2010; Grachev et al. 2013), and there is a persisting debate on the validity of the z-less stratification assumption (Yagüe et al. 2001; Grachev et al. 2005, 2013; Mahrt 2007; Hong 2010).

Using extensive observations over the Arctic pack ice, Grachev et al. (2013) reported that deviations from z-less theory were associated with non-Kolmogorov turbulence (i.e., turbulence without a well-defined inertial subrange), not expected to adhere to MOST in the first place. They suggested Ri_f (the flux Richardson number) $= 0.20-0.25$ as a primary threshold for the applicability of MOST, as they found inertial subrange slopes of velocity spectra to depart from $-5/3$ for $Ri_f > 0.20-0.25$. After filtering out the periods with Ri_f above the threshold, their results showed adherence to the z-less limit of MOST, and they concluded that this approach fully explains the controversy on the subject. In other words, the use of data periods characterized by non-Kolmogorov turbulence may explain why previous studies have found a MOST z-less breakdown, but those periods are not supposed to follow MOST in the first place (note that different screening/selection of periods may lead to different conclusions).

We used the Ri_f-based screening method in a first attempt ($Ri_f < 0.2$ specifically), and our results for S_{hr}^{+} and D^{+} indicated a close agreement with the linear MOST z-less prediction (even for $\zeta > 1$; results not shown), in agreement with the results of Grachev et al. (2013). However, note that this filtering method is justified only if the inertial subrange slope values depart from $-5/3$ for $Ri_f > 0.2$. The inertial subrange slope values we obtained for S_{uu}, different from the results in Grachev et al. (2013), did not display a clear relationship with Ri_f (data not shown). Many periods with Kolmogorov turbulence were observed for $Ri_f > 0.2$, and their removal was not justified. A different screening method was then adopted, based directly on the departure of the inertial subrange slope values from $-5/3$ (cf. Sect. 2.3). After using this more robust approach for our dataset, our results for S_{hr}^{+} (Fig. 5a) indicate z-less breakdown for $\zeta \gtrsim 1$. Our results indicate that the presence of Kolmogorov turbulence is not a sufficient criterion to guarantee the applicability of the MOST z-less concept, as suggested by Grachev et al. (2013).

Based on the results we obtained for the residual term, we hypothesize that an injection of non-local TKE to the 34–68-m layer via pressure transport is responsible for the z-less breakdown observed for S_{hr}^{+} at high stabilities. Obviously, $T_p^{+} \neq 0$, per se, would already be a sign of z-less breakdown. It is possible that such turbulence has an 'inactive' nature (Högström 1990), i.e., consisted of large-scale fluctuations contributing to the increasing of mixing (standard deviations) but not to the transport of momentum (u_*).

Both S_{hr}^{+} and R^{+} increase linearly with ζ up to $\zeta \approx 1$, and above that R^{+} increases faster with ζ, while S_{hr}^{+} increases at a slower rate. As discussed earlier, the effect of advection and accumulated errors on R^{+} is expected to be larger at higher stabilities, but if we assume that R^{+} represents mostly T_{p}^{+}, the increase of mixing due to the injection of 'inactive' turbulence via T_{p}^{+} could lead to a decrease in the wind-speed gradient and therefore to the decrease of S_{hr}^{+} in relation to the linear z-less prediction, observed for $\zeta \gtrsim 1$. It is interesting to observe that the dissipation term (Fig. 5b), calculated based on spectral densities in the inertial subrange (small eddy scales), seems to approximately follow the linear z-less prediction for $\zeta > 1$. This implies that the total energy gain in the considered layer (i.e., via S_{hr}^{+} and R^{+}) should be linear with ζ.

4 Conclusions

The behaviour of near-surface turbulence during nocturnal LLJ events was investigated using a combination of sodar and flux-tower data collected in the upper coastal plains of South Carolina, USA over a three-month period. The analysis focused on the TKE budget near the surface, with special attention to the pressure transport term, and also on the applicability of MOST. Cases with well-developed turbulence were selected for the analysis.

The near-surface TKE budget was found to be locally imbalanced, opposing the classic view of the TKE budget in the SBL. The total local energy losses (buoyant consumption and dissipation) were found to typically exceed local shear production, implying an input of non-local TKE. As the turbulent transport term was found to be practically negligible, the observed additional TKE was attributed to pressure transport and advection, calculated together as a residual term of the budget. The residual was found to be in approximate balance with buoyant consumption. Based on a comparison with previous results in the literature, it was hypothesized that this residual term represented mostly pressure transport.

Previous findings on the near-surface TKE budget in the presence of LLJs also indicate that the turbulent transport is very small, but results for the pressure transport vary (cf. Table 1). It is important to note first that the differences observed across studies could be at least in part related to different approaches used in the calculation of T_{p}. The great majority of studies on TKE budget in the atmospheric boundary layer, the current study included, use the residual approach to calculate T_{p}. An obvious limitation of this method is that the residual term may include advection (typically assumed negligible, but may vary from site to site) and accumulated errors, which may vary depending on the available measurements and the method used to process the turbulence data.

The general view in previous studies is that TKE is transported away from layers of maximum shear production (at the surface or close to the LLJ core) by pressure transport, but results from studies including Högström (1990), Smedman et al. (1993), and Bergström and Smedman (1995) indicate that TKE may be transported from upper regions in the boundary layer, in a process not necessarily associated with LLJs. In the present study, the behaviour of T_{p} (assumed to be approximately represented by the residual term) was generally similar for periods with and without LLJs, suggesting an upward transport of TKE from a layer of maximum shear production near the surface (as in Smedman et al. 1995 and Cuxart et al. 2002), or more likely, a downward transport from upper regions in the boundary layer. Under LLJ conditions, however, the behaviour of T_{p} was found to be better delineated, with a closer balance between T_{p} and buoyant consumption.

The shear production and dissipation terms during LLJs were found to conform well to the MOST local z-less predictions in general, corroborating earlier findings by Cheng et al. (2005), with the support of a more extensive dataset. Under very stable conditions, however, shear production was found to depart from the linear prediction. This result indicates that the presence of Kolmogorov turbulence (i.e., well-developed turbulence with inertial subrange slope close to $-5/3$) is not a sufficient condition to guarantee the applicability of the MOST z-less concept, as suggested by Grachev et al. (2013).

It is hypothesized that a gain of non-local TKE via pressure transport (per se an indication of conflict with the z-less concept) is the cause of the observed behaviour for S_{hr}^{+} under very stable conditions (values smaller than the z-less prediction). Such energy, likely of an 'inactive' nature, would affect mixing (by increasing the variance of the velocity components) but not directly u_*, as discussed in Högström (1990). The enhanced mixing would reduce the wind-speed gradient, and therefore S_{hr}^{+}.

Of relevance to numerical modelling studies of the SBL, the results presented in this study suggest that pressure transport cannot be neglected in the TKE budget. The processes controlling this term remain uncertain. Until a new sensor technology emerges allowing a direct and accurate calculation of the pressure transport term, further studies investigating T_{p} in the SBL via the residual approach using long data records (i.e., not restricted to a case study) would help advance the understanding of this term. Despite the limitations of the residual approach, the emergence of a pattern across different studies would be enlightening.

The present study also found that turbulence during LLJ periods was typically stronger and more well-developed, with an improved and well-defined inertial subrange in comparison with periods without a LLJ. This result has an important implication to flux-tower measurements of local net ecosystem exchange during nighttime stable conditions. It suggests that the use of a u_* threshold criterion (a common approach in the eddy-flux community—see Aubinet et al. 2012) most likely would result in a selection of periods under the influence of LLJs (average u_* was found to be 39 % larger for the LLJ group). LLJs may provide the turbulent conditions necessary for calculating fluxes via the eddy-covariance technique, but that does not guarantee that the advective terms contributing to the net ecosystem exchange are negligible (see also Hong et al. 2012). In fact, the LLJs may actually accentuate the advection terms. Neglecting those terms in that case could result in significant errors in the measurements of net ecosystem exchange. This approximation is made in most studies, given the extreme difficulties of measuring advection in the field.

Acknowledgments The authors gratefully acknowledge the comments of Nelson Dias, Carmen Nappo, and three anonymous reviewers, who helped to improve the quality of the manuscript. This study was funded by the U.S. Department of Energy, Terrestrial Carbon Processes Program, grant ER64321. The work performed by SRNL was supported, in part, from funding also provided by the DOE Office of Science—Terrestrial Carbon Processes Program and was performed under contract no. DE-AC09-08SR22470.

References

Aubinet M, Vesala T, Papale D (eds) (2012) Eddy covariance—a practical guide to measurement and data analysis. Springer, Dordrecht, 438 pp

Axelsen SL, Dop HV (2009) Large-eddy simulation of katabatic winds. Part 2: sensitivity study and comparison with analytical models. Acta Geophys 57:837–856

Banta RM (2008) Stable-boundary-layer regimes from the perspective of the low-level jet. Acta Geophys 56:58–87

Banta RM, Newsom RK, Lundquist JK, Pichugina YL, Coulter RL, Mahrt L (2002) Nocturnal low-level jet characteristic over Kansas during CASES-99. Boundary-Layer Meteorol 105:221–252

Banta RM, Pichugina YL, Newsom RK (2003) Relationship between low-level jet properties and turbulence kinetic energy in the nocturnal stable boundary layer. J Atmos Sci 60:2549–2555
Banta RM, Pichugina YL, Brewer WA (2006) Turbulent velocity-variance profiles in the stable boundary layer generated by a nocturnal low-level jet. J Atmos Sci 63:2700–2719
Batchelor GK (1953) The theory of homogeneous turbulence. Cambridge University Press, Cambridge 197 pp
Bergström H, Smedman A-S (1995) Stably stratified flow in a marine atmospheric surface layer. Boundary-Layer Meteorol 72:239–265
Blackadar AK (1957) Boundary layer wind maxima and their significance for the growth of nocturnal inversions. Bull Am Meteorol Soc 38:283–290
Businger JA, Wyngaard JC, Isumi Y, Bradley EF (1971) Flux–profile relationships in the atmospheric surface layer. J Atmos Sci 28:181–189
Cheng Y, Parlange MB, Brutsaert W (2005) Pathology of Monin–Obukhov similarity in the stable boundary layer. J Geophys Res 110:D06101
Conangla L, Cuxart J (2006) On the turbulence in the upper part of the low-level jet: an experimental and numerical study. Boundary-Layer Meteorol 118:379–400
Corsmeier U, Kalthoff N, Kolle O, Kotzian M, Fiedler F (1997) Ozone concentration jump in the stable nocturnal boundary layer during a LLJ-event. Atmos Environ 31:1977–1989
Cuxart J, Jiménez MA (2007) Mixing processes in a nocturnal low-level jet: an LES study. J Atmos Sci 64:1666–1679
Cuxart J, Morales G, Terradellas E, Yagüe C (2002) Study of coherent structures and estimation of the pressure transport terms for the nocturnal stable boundary layer. Boundary-Layer Meteorol 105:305–328
Doyle JD, Warner TT (1993) A three-dimensional numerical investigation of a Carolina coastal low-level jet during GALE IOP 2. Mon Weather Rev 121:1030–1047
Duarte HF, Leclerc MY, Zhang G (2012) Assessing the shear-sheltering theory applied to low-level jets in the nocturnal stable boundary layer. Theor Appl Climatol 110:359–371
Dyer AJ (1974) A review of flux–profile relationships. Boundary-Layer Meteorol 7:363–372
Foken T, Meixner FX, Falge E, Zetzsch C, Serafimovich A, Bargsten A, Behrendt T, Biermann T, Breuninger C, Dix S, Gerken T, Hunner M, Lehmann-Pape L, Hens K, Jocher G, Kesselmeier J, Lüers J, Mayer JC, Moravek A, Plake D, Riederer M, Rütz F, Scheibe M, Siebicke L, Sörgel M, Staudt K, Trebs I, Tsokankunku A, Welling M, Wolff V, Zhu Z (2012) Coupling processes and exchange of energy and reactive and non-reactive trace gases at a forest site: results of the EGER experiment. Atmos Chem Phys 12:1923–1950
Frenzen P, Vogel CA (2001) Further studies of atmospheric turbulence in layers near the surface: scaling the TKE budget above the roughness sublayer. Boundary-Layer Meteorol 99:173–206
Grachev AA, Fairall CW, Persson POG, Andreas EL, Guest PS (2005) Stable boundary-layer scaling regimes: the Sheba data. Boundary-Layer Meteorol 116:201–235
Grachev AA, Andreas EL, Fairall CW, Guest PS, Persson POG (2013) The critical Richardson number and limits of applicability of local similarity theory in the stable boundary layer. Boundary-Layer Meteorol 147:51–82
Högström U (1990) Analysis of turbulence structure in the surface layer with a modified similarity formulation for near neutral conditions. J Atmos Sci 47:1949–1972
Högström U (1992) Further evidence of 'inactive' turbulence in the near neutral atmospheric surface layer. In: 10th symposium on turbulence and diffusion, Portland, OR, American Meteorological Society, Boston, pp 188–191
Hong J (2010) Note on turbulence statistics in z-less stratification. Asia-Pacific J Atmos Sci 46:113–117
Hong J, Mathieu N, Strachan IB, Pattey E, Leclerc MY (2012) Response of ecosystem carbon and water vapor exchanges in evolving nocturnal low-level jets. Asian J Atmos Environ 6:222–233
Kaimal JC, Finnigan JJ (1994) Atmospheric boundary layer flows. Oxford University Press, New York, 289 pp
Karipot A, Leclerc MY, Zhang G, Martin T, Starr G, Hollinger D, McCaughey JH, Hendrey GR (2006) Nocturnal CO_2 exchange over a tall forest canopy associated with intermittent low-level jet activity. Theor Appl Climatol 85:243–248
Karipot A, Leclerc MY, Zhang G, Lewin KF, Nagy J, Hendrey GR, Starr G (2008) Influence of nocturnal low-level jet on turbulence structure and CO_2 flux measurements over a forest canopy. J Geophys Res 113:D10102
Karipot A, Leclerc MY, Zhang G (2009) Climatology of the nocturnal low-level jets observed over north Florida. Mon Weather Rev 137:2605–2621
Li X, Zimmerman N, Princevac M (2008) Local imbalance of turbulent kinetic energy in the surface layer. Boundary-Layer Meteorol 129:115–136

Mahrt L (1999) Stratified atmospheric boundary layers. Boundary-Layer Meteorol 90:375–396
Mahrt L (2007) The influence of nonstationarity on the turbulent flux–gradient relationship for stable stratification. Boundary-Layer Meteorol 125:245–264
Mahrt L, Vickers D (2002) Contrasting vertical structures of nocturnal boundary layers. Boundary-Layer Meteorol 105:351–363
Mahrt L, Heald RC, Lenschow DH, Stankov BB, Troen I (1979) An observational study of the structure of the nocturnal boundary layer. Boundary-Layer Meteorol 17:247–264
Mastrantonio G, Einaudi F, Fua D (1976) Generation of gravity waves by jet streams in the atmosphere. J Atmos Sci 33:1730–1738
May PT (1995) The Australian nocturnal jet and diurnal variations of boundary-layer winds over Mt. Isa in north-eastern Australia. Q J R Meteorol Soc 121:987–1003
McBean GA, Elliot JA (1975) Vertical transports of kinetic energy by turbulence and pressure in the boundary layer. J Atmos Sci 32:753–766
Muñoz RC, Garreaud RD (2005) Dynamics of the low-level jet off the west coast of subtropical South America. Mon Weather Rev 133:3661–3677
Oncley SP, Friehe CA, LaRue JC, Businger JA, Itsweire EC, Chang SS (1996) Surface-layer fluxes, profiles, and turbulent measurements over uniform terrain under near-neutral conditions. J Atmos Sci 53:1029–1044
Piper M, Lundquist JK (2004) Surface layer turbulence measurements during a frontal passage. J Atmos Sci 61:1768–1780
Rannik Ü, Vesala T (1999) Autoregressive filtering versus linear detrending in estimation of fluxes by the eddy covariance method. Boundary-Layer Meteorol 91:259–280
Shuqing S (1985) Gravity waves on the axis of low level jet and their instability. Adv Atmos Sci 2:112–123
Sjostedt DW, Sigmon JT, Colucci SJ (1990) The Carolina nocturnal low-level jet: synoptic climatology and a case study. Weather Forecast 5:404–415
Skyllingstad ED (2003) Large-eddy simulation of katabatic flows. Boundary-Layer Meteorol 106:217–243
Smedman A-S, Tjernström M, Högström U (1993) Analysis of the turbulence structure of a marine low-level jet. Boundary-Layer Meteorol 66:105–126
Smedman A-S, Tjernström M, Högström U (1994) The near-neutral marine atmospheric boundary layer with no surface shearing stress: a case study. J Atmos Sci 51:3399–3411
Smedman A-S, Bergström H, Högström U (1995) Spectra, variances and length scales in a marine stable boundary layer dominated by a low level jet. Boundary-Layer Meteorol 76:211–232
Sogachev A, Leclerc MY (2011) On concentration footprints for a tall tower in the presence of a nocturnal low-level jet. Agric For Meteorol 151:755–764
Song J, Liao K, Coulter RL, Lesht BM (2005) Climatology of the low-level jet at the Southern Great Plains Atmospheric Boundary Layer Experiments site. J Appl Meteorol 44:1593–1606
Stull RB (1988) An introduction to boundary layer meteorology. Kluwer, Dordrecht, 666 pp
Todd MC, Washington R, Raghavan S, Lizcano G, Knippertz P (2008) Regional model simulations of the Bodélé low-level jet of northern Chad during the Bodélé Dust Experiment (BoDEx 2005). J Clim 21:995–1012
Vera C, Baez J, Douglas M, Emmanuel CB, Marengo J, Meitin J, Nicolini M, Nogues-Paegle J, Paegle J, Penalba O, Salio P, Saulo C, Silva Dias MA, Silva Dias P, Zipser E (2006) The South American low-level jet experiment. Bull Am Meteorol Soc 87:63–77
Vickers D, Mahrt L (1997) Quality control and flux sampling problems for tower and aircraft data. J Atmos Ocean Technol 14:512–526
Wang D, Zhang Y, Huang A (2013) Climatic features of the south-westerly low-level jet over southeast China and its association with precipitation over east China. Asia-Pacific J Atmos Sci 49:259–270
Wang Y, Creegan E, Felton M, Ligon D, Huynh G (2013) Investigation of nocturnal low-level jet-generated gravity waves over Oklahoma City during morning boundary layer transition period using Doppler wind lidar data. J Appl Remote Sens 7:073487
Wilczak JM, Oncley SP, Stage SA (2001) Sonic anemometer tilt correction algorithms. Boundary-Layer Meteorol 99:127–150
Wyngaard JC (2010) Turbulence in the atmosphere. Cambridge University Press, Cambridge, 393 pp
Wyngaard JC, Coté OR (1971) The budget of turbulent kinetic energy and temperature variance in the atmospheric surface layer. J Atmos Sci 28:190–201
Yagüe C, Maqueda G, Rees JM (2001) Characteristics of turbulence in the lower atmosphere at Halley IV station, Antarctica. Dyn Atmos Oceans 34:205–223
Zhang D, Zhang S, Weaver SJ (2006) Low-level jets over the mid-Atlantic States: warm-season climatology and a case study. J Appl Meteorol Climatol 45:194–209